Applied Catalysis B: Environmental 245 (2019) 40–48

Contents lists available at ScienceDirect

Applied Catalysis B: Environmental

journal homepage: www.elsevier.com/locate/apcatb

From alumina modified Rh/$Ce_{0.75}Zr_{0.25}O_{2-\delta}$ catalyst towards composite Rh/$Ce_{0.75}Zr_{0.25}O_{2-\delta}$-η-$Al_2O_3$/FeCrAl catalytic system for diesel conversion to syngas

T.B. Shoynkhorova[a], P.V. Snytnikov[a,b,c,*], P.A. Simonov[a,c], D.I. Potemkin[a,b], V.N. Rogozhnikov[a], E.Y. Gerasimov[a], A.N. Salanov[a], V.D. Belyaev[a,b,c], V.A. Sobyanin[a,*]

[a] Boreskov Institute of Catalysis, Pr. Akademika Lavrentieva, 5, Novosibirsk, 630090, Russia
[b] Novosibirsk State University, Pirogova St., 2, Novosibirsk, 630090, Russia
[c] UNICAT Ltd, Pr. Akademika Lavrentieva, 5, Novosibirsk, 630090, Russia

ARTICLE INFO

Keywords:
Steam conversion
Autothermal reforming
Diesel
Hexadecane
Rhodium
Alumina
Ceria-zirconia
Structured catalyst
Hydrogen-rich stream
Syngas
Wire metal mesh

ABSTRACT

It was investigated how the modification of $Ce_{1-x}Zr_xO_{2-\delta}$ with alumina as structural additive affected the surface characteristics of the support. The effect of alkaline promoters on the catalyst coking resistance and activity was studied. Sorption-hydrolytic deposition technique was used to prepare a set of catalysts containing 1 wt.% Rh deposited on Al_2O_3 - $Ce_{0.75}Zr_{0.25}O_{2-\delta}$, $Ce_{0.75}Zr_{0.25}O_{2-\delta}$ and Al_2O_3 - $Ce_{0.75}Zr_{0.25}O_{2-\delta}$, doped with alkaline metal. The catalysts were characterized by BET, TEM, SEM, XRD, TPO, and CO chemisorption methods. It was proved that the catalysts contained high-dispersion Rh particles of size 1–2 nm. The presence of Al deteriorated catalytic activity of Rh/ Al_2O_3 - $Ce_{0.75}Zr_{0.25}O_{2-\delta}$ for steam reforming of diesel surrogate (n-hexadecane) at T = 550 °C, H_2O/C = 3.0, GHSV = 20,000 h^{-1}, whereas the alkaline additives promoted n-hexadecane steam reforming. Rh/$Ce_{0.75}Zr_{0.25}O_{2-\delta}$ appeared to be the most stable catalyst, as it provided 100% conversion of n-hexadecane during 15 h on stream. The active component Rh/$Ce_{0.75}Zr_{0.25}O_{2-\delta}$ was supported on FeCrAl alloy wire mesh using alumina as a binding structural component. The obtained catalyst Rh/$Ce_{0.75}Zr_{0.25}O_{2-\delta}$-η-$Al_2O_3$/FeCrAl was tested in the autothermal reforming of n-hexadecane at various temperatures and gas flow rates. Operating conditions were found to provide a 100% conversion of n-hexadecane and stable catalyst activity.

1. Introduction

The development of highly efficient modular power generation units is of great importance. Solid oxide fuel cells (SOFC) are currently considered as the most efficient devices for the conversion of hydrocarbons (natural gas, LPG, JP or diesel) into electric power. To provide stable SOFC operation, initial fuel, before feeding to the SOFC anode, should be converted to synthesis gas with high content of hydrogen [1]. Catalytic steam (SR), combined steam-dry (SDR), partial oxidation (PO) or autothermal reforming (ATR) are the most appropriate reactions for this purpose. The optimum temperature for these reactions is 550–900 °C, which falls within the SOFC working temperature range.

Diesel fuel is a promising substance for the conversion into a hydrogen-rich gas suitable for SOFC feeding due to its readily available infrastructure and wide application scope. There are a lot of publications devoted to the studies of oxidative reforming of diesel fuel with particular focus on the development of efficient catalysts based on noble metals (Rh, Ru, Pt) or Ni. As shown in a number of works [2–6], Rh-based catalysts demonstrate high activity and selectivity for hydrogen-rich gas production both in lab and short term pilot scale experiments. However, in the hundred hours time-on-stream experiments, gradual decrease of catalyst performance (diesel conversion and syngas productivity) is usually observed owing to undesired processes of coke formation by the reactions on the catalyst surface and homogeneous thermocracking reactions producing light unsaturated hydrocarbons (such as ethylene [7]), sulfur poisoning, segregation of the catalyst active component. In addition to the efforts to solve these problems, considerable attention is focused on minimizing the loading of expensive rhodium by improving the catalyst performance. Moreover, the diesel reforming catalysts require high intrinsic heat conductivity to provide uniform temperature distribution in the case of highly endothermal SR and effective heat redistribution in the case of ATR and PO processes. One of the proposed solutions is to deposit a thin catalytic coating onto ceramic or metal honeycomb carriers [8–10]. Substrates

* Corresponding authors at: Boreskov Institute of Catalysis, Pr. Akademika Lavrentieva, 5, Novosibirsk, 630090, Russia.
E-mail addresses: pvsnyt@catalysis.ru (P.V. Snytnikov), sobyanin@catalysis.ru (V.A. Sobyanin).

https://doi.org/10.1016/j.apcatb.2018.12.037
Received 1 August 2018; Received in revised form 16 November 2018; Accepted 14 December 2018
Available online 15 December 2018
0926-3373/ © 2018 Elsevier B.V. All rights reserved.

made of metal wire meshes and foams seem to be promising due to sufficient heat conductivity, but conventional coating approach based on suspension binding to metal substrates suffers from non-uniformity and weak adhesion [8]. Another promising strategy is based on the modified Bayer process which allows to cover the overall surface of the FeCrAl alloy metal wire mesh by strongly bound η-Al_2O_3 layer [10] which has high specific surface area (S_{BET} ~240 m^2/g) and mechanical strength. The layer is a needle-type structure of 10–20 μm height, which forms the surface micro-roughness. Calcination of η-Al_2O_3 layer higher than 850 °C leads to its transformation into θ-Al_2O_3 with a lower specific surface area (S_{BET} ~60 m^2/g). Alumina is known [11–13] as an efficient binding component owing to its thermal stability and low cost. However, alumina in the diesel reforming catalyst may cause undesirable catalyst coking due to the presence of acid sites. As for the high-temperature phase α-Al_2O_3, it has low specific surface area that hinders its application for preparation of highly active catalysts.

The use of cerium-containing materials is promising because cerium ions can undergo partial reduction and oxidation in response to variation of oxygen concentration in the gas phase. This property, which is characterized by oxygen storage capacity (OSC), minimizes the coke formation. Zirconia additive improves the catalyst thermal stability, as it prevents the decrease in CeO_2 specific surface area, and increases OSC [3,14]. It was demonstrated that CeO_2 doping by transition metals (including rhodium) increases ceria OSC as well [15]. It was shown also that the uniform mixing of Al_2O_3 and $Ce_{0.75}Zr_{0.25}O_{2-\delta}$ particles on the nanometer scale enhanced the sintering resistance of the composite [16]. Alumina served as a structural promoter and diffusion barrier for the $Ce_{0.75}Zr_{0.25}O_{2-\delta}$ particles. The results of the promoting effect were the increased thermal stability, high OSC, and high activity of the catalysts supported on this composite.

In our previous study [6], three noble metal catalysts (Rh-, Pt-, Ru/$Ce_{0.75}Zr_{0.25}O_{2-\delta}$) for reforming of hydrocarbons were examined in steam and autothermal process conditions. It was shown that Rh-based catalyst synthesized by sorption-hydrolytic deposition surpassed in activity and stability the Ru- and Pt-based catalysts, as well as the Rh-based catalyst synthesized by incipient wetness impregnation technique.

The aim of the present work was to investigate how modification of $Ce_{0.75}Zr_{0.25}O_{2-\delta}$ with a structural additive Al_2O_3 affected the catalyst performance, and to study the effect of alkaline promoters on the catalyst coking resistance and activity in the autothermal and steam reforming of n-hexadecane (HD) used as a diesel surrogate. Sorption - hydrolytic deposition technique was used to prepare a set of catalysts containing 1 wt.% Rh. Additionally, structured Rh/$Ce_{0.75}Zr_{0.25}O_{2-\delta}$-η-$Al_2O_3$/FeCrAl wire metal mesh catalyst was prepared, characterized, and studied in HD ATR. Transmission Electron Microscopy (TEM), Scanning Electron Microscopy (SEM), BET, temperature-programmed oxidation (TPO), X -ray diffraction (XRD) and CO chemisorption analyses were used for catalyst characterization and coke formation studies.

2. Experimental

2.1. Catalyst preparation

Composite oxides $Ce_{0.75}Zr_{0.25}O_{2-\delta}$ (CZ) and $Ce_{0.75}Zr_{0.25}O_{2-\delta}$- Al_2O_3 with $Ce_{0.75}Zr_{0.25}O_{2-\delta}$ to Al_2O_3 weight ratio of 1:1 (CZA) with fluorite structure was purchased from Ecoalliance Ltd. (Russia). CZ and CZA were prepared by direct precipitation described in detail elsewhere [16]. Solutions of Ce^{3+}, ZrO^{2+} and Al^{3+} nitrates were combined in fixed proportions resulting in concentrations of components totaling 0.1 g cm^{-3}. The composite oxide was precipitated from the solution by adding 25% aqueous ammonia dropwise under permanent stirring. The mixtures were held at 100 °C and atmospheric pressure for 120 h. Thereafter, the precipitates were filtered and repulped in isopropanol. The resulting slurries were dried at 100 °C for 12 h and calcined at 500 °C for 2 h, and then at 800 °C for 1 h. The synthesized CZ and CZA materials were crashed in an agate mortar, and the 0.2–0.5 mm fraction was separated for further catalyst synthesis. Properties of CZ and CZA are described in detail elsewhere [16]. CZ and CZA specific surface areas (S_{BET}) were 69 and 145 m^2 g^{-1}, respectively.

CZA was kept in aqueous solution of $Mg(OAc)_2$ for 12 h, dried at 65 °C and calcined at 800 °C for 0.5 h. To remove unbound Mg, the support, hereafter CZA-Mg, was washed out with an aqueous solution of acetic acid, dried at 65 °C and calcined at 600 °C for 0.5 h. S_{BET} of CZA-Mg was 140 m^2 g^{-1}.

20 wt.% of pseudoboehmite was introduced to the $Ce_{0.75}Zr_{0.25}O_{2-\delta}$ powder as a binder, and the sample was calcined at 800 °C for 0.5 h. The resulted support was denoted as CZB. The synthesized CZB powder was pressed into pellets, crushed, and the 0.2-0.5 mm fraction was separated. S_{BET} of CZB was 120 m^2 g^{-1}.

The supported Rh/CZ, Rh/CZA, Rh/CZB and Rh/CZA-Mg catalysts with metal loading of 1 wt.% were prepared by a sorption-hydrolytic deposition technique according to [17] and described in detail elsewhere [6]. The main idea of this technical approach is to form a solution of "metal complex + alkaline agent" which is metastable at the given conditions (temperature, concentrations) with respect to homogeneous metal hydroxide precipitation. This is due to the kinetic inertness of the metal complexes for ligand exchange [18]. As the support surface accelerates heterogeneous nucleation and growth of metal hydroxide particles [19], addition of support to the reagent mixture initiates hydrolysis which leads to uniform depositing of the metals over the support surface.

For this purpose, a solution of $RhCl_3$ was mixed with Na_2CO_3 in a molar ratio of Na/Cl = 1. The mixture was then brought into contact with aqueous suspension of the CZ, CZA, CZB or CZA-Mg supports. The depositing was performed at 75 °C. After the end of the depositing procedure (i.e., when no reaction of the solution with $NaBH_4$ was observed), the samples were thoroughly rinsed with hot water by decanting, dried and reduced in a hydrogen flow at 250 °C for 30 min. S_{BET} of the prepared catalysts was close to that of the supports.

FeCrAl alloy wire mesh (0.5 x 0.5 mm, thickness 0.25 mm) with protective coating of 6 wt.% of η-Al_2O_3 prepared according to [11] was chosen as a substrate for catalyst deposition. The 12 wt.% $Ce_{0.75}Zr_{0.25}O_{2-\delta}$-η-$Al_2O_3$/FeCrAl (further denoted as CZB/FCA) structured support was prepared via 7-step impregnation of η-Al_2O_3 -coating by saturated solution of $Ce(NO_3)_3$•$6H_2O$ and $ZrO(NO_3)_2$•$2H_2O$ (Ce/Zr = 3) with intermediate thermal treatment at 800 °C for 5 min and final calcination for 0.5 h at the same temperature. The Rh/CZB/FCA catalysts was synthesized by depositing 0.24 wt.% of Rh onto CZB/FCA by the sorption-hydrolytic deposition technique described above.

2.2. Catalyst characterization

The BET specific surface area (S_{BET}) of the support, as-prepared and used catalysts was determined from the complete nitrogen adsorption isotherms at –196 °C using an ASAP 2400sorptometer (Micromeritics, USA).

The dispersion of the metal particles supported over CZ, CZA, CZB and CZA-Mg, their specific surface area and mean size were evaluated using pulse chemisorption of CO in H_2 at 20 °C, assuming that each surface metal atom adsorbs CO molecule at a ratio of 1.5. Prior to the CO chemisorption measurement, the catalysts were reduced in a hydrogen flow at 350 °C for 30 min. The technique of pulse titration of the metal surface was adopted from [20].

The X-ray diffraction (XRD) patterns were obtained on a diffractometer X'tra (Thermo Scientific, Switzerland) using monochromatic CuKα radiation (λ = 154.18 pm). The measurements were carried out in the 2θ range of 15–80 °C with a step of 0.05° and 5.0 s sampling time. The ICDD PDF-2 database was used for the phase composition analysis. The Rietveld refinement with quantitative phase analysis was performed using TOPAS v4.3 software. The sizes of the

coherent scattering regions (D_{XRD}) were calculated by line broadening analysis according to the Scherrer equation.

To quantify the carbon formation during steam and autothermal reforming of HD, the used catalysts were studied by TPO using a TG209 F1 LibraThermo microbalance instrument (Netzsch, Germany). The feed gas, 6 vol.% O_2 in He, flowed at a rate of 70 $cm^3\,min^{-1}$. The temperature was raised linearly from 30 to 900 °C at a rate of 10 °C min^{-1}. The outlet CO_2 concentration was monitored on-line using a QMC-200 mass-spectrometer (Stanford Research Systems, USA).

The transmission electron microscopy (TEM) images of the as-prepared and used catalysts were obtained using a JEOL JEM 2010 electron microscope with 1.4 Å resolution at 200 kV (JEOL Ltd., Japan). The interplanar spacing was analyzed, and the particles composition was determined using a JCPDS-ICDD database. To prepare the sample for characterization, a portion of the catalytic coating of Rh/CZB/FCA catalyst was scraped off the FeCrAl alloy wire mesh.

Rh/CZB/FCA catalyst was studied by scanning electron microscopy (SEM) technique using a scanning electron microscope SM-6460 LV (JEOL Ltd., Japan). Cross sections of sample were made by pouring the sample with epoxy resin followed by multistep polishing. The surface chemical composition of the studied samples was determined by Energy Dispersive X-ray Microanalysis (EDX) using an INCAEnergy-350 instrument (Oxford Instruments, Great Britain). Test samples were previously coated with 20 nm thick carbon film to reduce noise in the micrographs caused by the effects of samples charging. Micrographs were obtained with the electron energy of 20 keV. To analyze the surface morphology, the images were obtained in the detection mode of secondary electrons. To distinguish the regions with the different phase composition, the backscattered electrons were recorded.

2.3. Catalytic activity measurements

The reactions of n-hexadecane (Komponent-Reaktiv LLC, Russia) steam and autothermal reforming were performed in a fixed-bed continuous-flow U-shaped quartz reactor (ID: 7 mm) at atmospheric pressure in the temperature range of 550–650 °C. In all experiments, a 50 mm piece of copper foam, which served as an evaporator at 450 °C, was placed at the reactor inlet. The 130 mm space between the evaporator and the catalyst bed was filled with 1–2 mm quartz pellets homogenizing the reactants mixture. The fuel was fed via a capillary into the evaporator. The evaporated water from a steam generator together with the nitrogen carrier gas was supplied via a heated capillary to the evaporator and mixed with the vaporized fuel. Air was fed via a coaxially positioned capillary close to the catalyst bed. The reaction temperature was measured by a K-type thermocouple in the middle of the catalyst bed.

Prior to the experiments, the catalyst was reduced inside the reactor in a mixture of 10 vol. % H_2 in Ar at a heating rate of 6 °C min^{-1} up to 600 °C. The temperature was then changed to 550, 600 or 650 °C, and the reaction mixtures were fed to the reactor. The mixture compositions and catalyst loading were set respectively for each of the processes studied as follows:

- steam reforming: HD 1.6 g h^{-1}, H_2O 6 g h^{-1}; N_2 1800 cm^3 h^{-1} making the ratio $H_2O/C = 3$ at the gas hour space velocity (GHSV) of 20,000 h^{-1};
- autothermal reforming: HD 1.6 g h^{-1}, H_2O 5.3 g h^{-1}, air 6000 $cm^3\,h^{-1}$ making the ratios $H_2O/C = 2.6$, $O_2/C = 0.5$ at GHSV of 27,000 h^{-1};
- autothermal reforming over Rh/CZB/FCA: HD 0.8 - 2.4 g h^{-1}, H_2O 2.7 - 8.1 g h^{-1}, air - 3000 - 9000 $cm^3\,h^{-1}$ making the ratios $H_2O/C = 2.6$, $O_2/C = 0.4$ at the weight hourly space velocity (WHSV) in the range of 38,500 to 115,500 $cm^3\,g^{-1}\,h^{-1}$; WHSV was calculated as the ratio of total feed flow rate to the weight of catalyst coating. GHSV and WHSV were calculated at 25 °C and P = 1 atm.

The reformates were analyzed using a GC-1000 gas chromatograph (Chromos, Russia) equipped with a thermal conductivity detector (TCD) and a flame ionization detector (FID) with methanator. Before analysis, water was removed from the reformate using a moisture trap. Concentrations of H_2 and N_2 separated in a CaA column with an Ar carrier gas were determined with TCD. The CO, CO_2, CH_4, and C_2-C_5 hydrocarbons were separated in a Chromosorb 106 column and quantified using FID. Conversion of HD (X_{HD}) was determined gravimetrically every hour by collecting unreacted HD at the reactor condenser. It was calculated by the following equation:

$$X_{HD}\,(\%) = \frac{V_0 \bullet t - m_1}{V_0 \bullet t} \bullet 100,$$

where V_0 is the inlet mass flow of HD ($g \cdot h^{-1}$), t is the time of probe collecting (h), m_1 is the probe weight of unreacted HD (g), respectively.

Blank tests were performed as well. For this purpose, the reactor, instead of catalyst, was loaded with quartz pellets of the catalyst-size fraction (0.2-0.5 mm). In the blank tests, neither HD conversion ($X_{HD} = 0$), nor carbon formation were observed. These facts prove that the reactor design allowed minimization of the gas-phase homogeneous processes of HD thermal hydro cracking.

Thermodynamic equilibrium compositions of HD steam and autothermal reforming were calculated using HSC Chemistry software 7.0 and were used as reference data for interpreting the experimental results.

3. Results and discussion

3.1. Catalyst characterization

Fig. 1 presents the XRD patterns of the CZ, CZA supports and as-prepared Rh/CZ, Rh/CZA, Rh/CZB and Rh/CZA-Mg catalysts. The patterns of CZ and Rh/CZ samples contain the peaks corresponding to $Ce_{1-x}Zr_xO_2$ solid solution with a fluorite structure. The patterns of CZA, Rh/CZA, Rh/CZB and Rh/CZA-Mg demonstrate additional peaks attributed to γ-Al_2O_3. As the Rh loading in the catalysts was low, no peaks corresponding to metallic Rh was observed. Lattice parameters and the size of the coherent-scattering regions of $Ce_{1-x}Zr_xO_{2-\delta}$ solid solution for CZ and CZA were a = 5.385, 5.356 Å and D = 110 and 90 Å, respectively. These values remained the same for the samples with 1 wt.% Rh loading.

According to CO chemisorption data, the average size of Rh particles in all as-prepared catalysts was ~1 nm. These data agree well with the TEM results exemplified by the images of as-prepared and used Rh/CZ, Rh/CZB, Rh/CZA catalysts (Fig. 2). Clearly, all the samples contain highly dispersed Rh particles on the support surface predominantly in

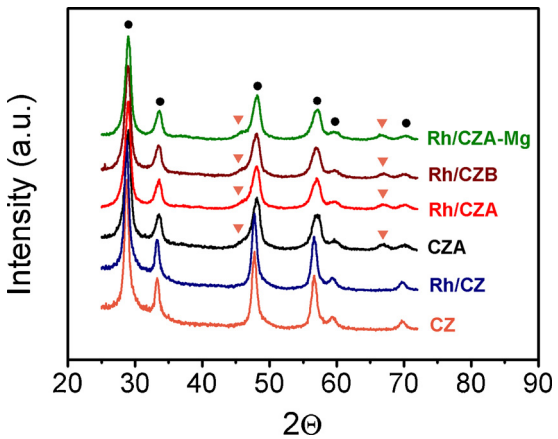

Fig. 1. XRD patterns of the CZ, CZA supports and as-prepared Rh/CZ, Rh/CZA, Rh/CZB and Rh/CZA-Mg catalysts; (●) - peaks corresponding to fluorite structure, (▼) – peaks corresponding to γ-Al_2O_3.

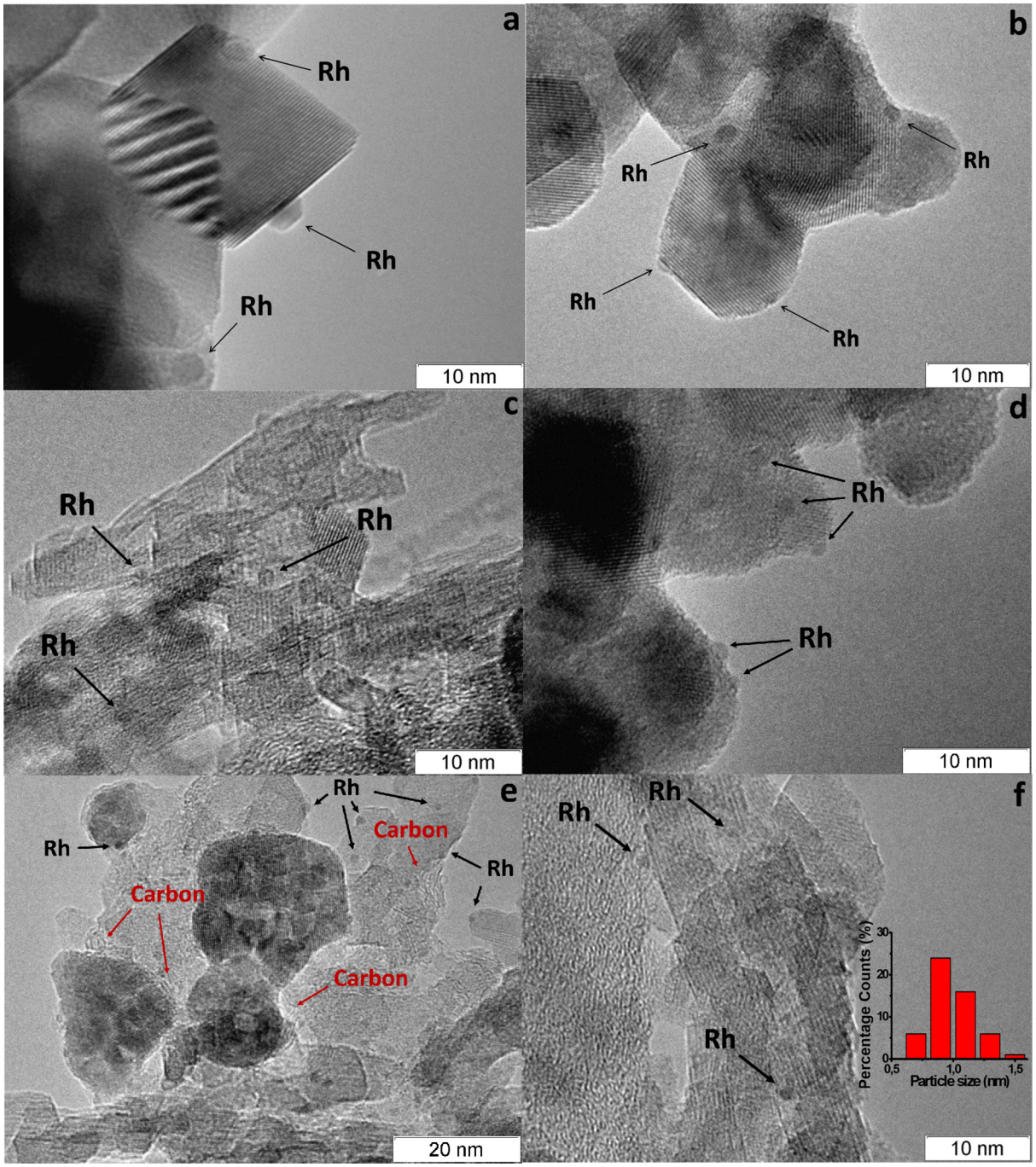

Fig. 2. TEM images of as-prepared Rh/CZ (a), Rh/CZB (c) and used in HD SR Rh/CZ (b), Rh/CZB (d), Rh/CZA (e) and annealed Rh/CZA (f) catalysts.

the form of 1–2 nm clusters. Some 2–3 nm particles with interplanar distances d = 2.196 Å and d = 1.902 Å corresponding to {111} and {200} planes, respectively, were observed as well. As Fig. 2e shows, Rh/CZA catalyst after HD SR contains carbon deposits. After oxidative treatment of the catalyst, the carbon deposits disappeared, while the size of Rh particles remained unchanged (Fig. 2f). As is seen from the TEM images, the CZ and Al_2O_3 phases do not form a single matrix. Compared to Al_2O_3, phase CZ exhibits highly regular, crystalline, sharp-edged structure. Rh particles locate both on CZ and Al_2O_3 surface.

The TPO data agree with the results of catalytic activity studies (See Section 3.2) and TEM data.

As Table 1 shows, Rh/CZA is the most susceptible to coking: it accumulated 3.7 wt.% of carbon in 12 h of HD SR. Since the size of Rh particles in Rh/CZA after annealing remains unchanged (Fig. 2f), rapid

Table 1
Carbon contents in the catalysts after HD SR and ATR.

Catalyst	Reaction	C, wt.%	Time on stream, h	P[a] ($g_C \cdot kg_{HD}^{-1} \cdot g_{cat}^{-1}$)
Rh/CZ	HD SR	1.2	15	0.5
Rh/CZA-Mg	HD SR	1.3	12	0.7
Rh/CZB	HD SR	2.3	15	1.0
Rh/CZA	HD SR	3.7	12	1.9
Rh/CZB	HD ATR	2.3	12	1.2
Rh/CZ	HD ATR	1.5	12	0.8
Rh/CZB/FCA	HD ATR	1.5[b]	27	0.3[b]

[a] P - the average carbon productivity during reaction per catalyst weight and weight of supplied HD.
[b] calculated with respect to catalyst coating weight.

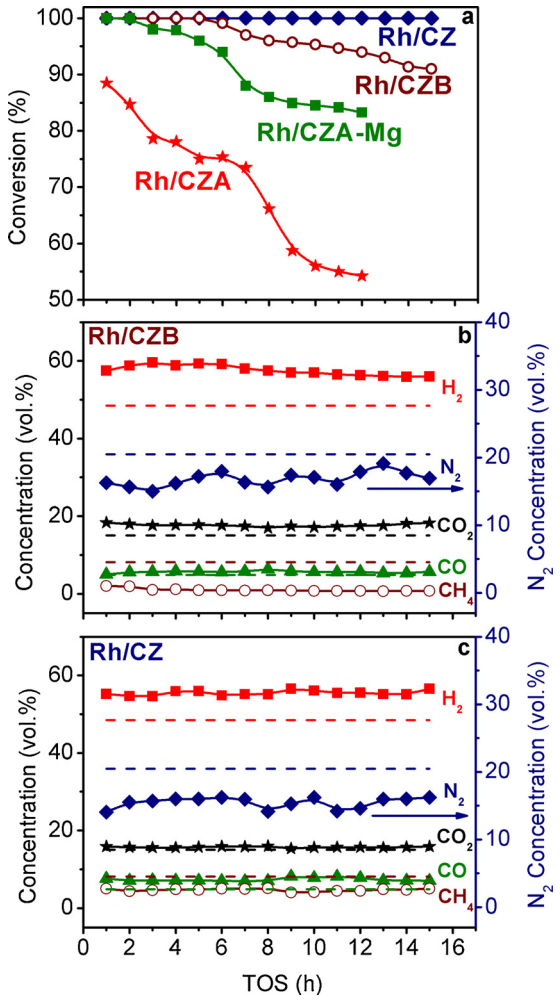

Fig. 3. The HD conversion (a) and product distribution on dry basis (b,c) over Rh/CZA, Rh/CZA-Mg, Rh/CZB and Rh/CZ in the HD SR as a function of time on stream at H_2O/C = 3.0, T = 550 °C and GHSV = 20,000 h^{-1}. Points – experimental data, dashed lines – equilibrium concentrations.

deactivation of the catalyst is explained by coke formation. As known, γ-Al_2O_3 contains acid sites, which are responsible for coke formation [21,22]. As proved by the results of Rh/CZA-Mg catalytic activity tests (Fig. 3a) and TPO data (Table 1), the blocking of acid sites by Mg cations causes a threefold decrease in the amount of the carbon formed. Compared to Rh/CZA-Mg and Rh/CZA, the use of 20 wt.% pseudoboehmite as a binder in Rh/CZB improves the catalyst performance in HD SR (Fig. 3 a,b), but the carbon productivity (P) exceeds that of Rh/CZA-Mg. The same amount of carbon was observed in Rh/CZB after HD ATR. This observation is associated with the Rh/CZB preparation procedure (see Section 2.1), when pseudoboehmite transformed to γ-Al_2O_3 under annealing, as proved by the XRD data (Fig. 1). Among the studied catalysts, Rh/CZ accumulated the lowest amount of carbon: 1.2 wt.% for 15 h of HD SR and 1.5 wt.% for 12 h of HD ATR. Low coke amount (1.5 wt.%) with average productivity of 0.3 $g_C \cdot kg_{HD}^{-1} \cdot g_{cat}^{-1}$ was identified by TPO over Rh/CZB/FCA after 27 h on stream. Rh/$Ce_{0.75}Zr_{0.25}O_2$-δ/η-Al_2O_3 catalytic coating was stable after 27 h on stream, no coating degradation was observed.

3.2. Steam reforming

Fig. 3a illustrates the effect of time on stream on HD conversion at HD SR over the Rh/CZA, Rh/CZA-Mg, Rh/CZB and Rh/CZ catalysts in a continuous-flow reactor. One can see that Rh/CZA demonstrated the worse HD SR performance. At 550 °C, complete HD conversion was not reached, during 12 h the conversion decreased from 89 to 54%. The main reaction products were H_2, CO_2, CO and CH_4; during the experiment, the concentrations of these compounds decreased, respectively, from 59 to 50, from 17 to 15, from 5 to 3 vol.% and CH_4 was approximately 0.2 vol.% (see Supplementary information for details). Total outlet concentration of C_2-C_5 hydrocarbons did not exceed 0.2 vol. %, and increased slightly with decreasing HD conversion.

It is seen that, in contrast to Rh/CZA, Rh/CZA-Mg provides 100% HD conversion, which, however, gradually decreases to 83% during 12 h. Concentrations of H_2, CO_2, CO and CH_4 decreased during the experiment from 57 to 45, from 19 to 17, from 5 to 4, from 3 to 0.2 vol. %, respectively (See Supplementary information). This process was accompanied by the raise of the outlet concentration of C_2-C_5 hydrocarbons.

During first 5 h on stream, Rh/CZB provided complete HD conversion (Fig. 3a). The products distribution (H_2, CO_2, CO and CH_4) slightly differed from the calculated equilibrium data (Fig. 3b). Only traces of the outlet C_2 - C_5 hydrocarbons were detected.

Slight deviation between the observed and equilibrium concentrations can be explained by the fact that methane is a secondary product that is formed from hydrogen and carbon oxides. The equilibrium concentrations are not reached for this catalyst at the given space velocity.

For the next 10 h, the catalyst gradually lost its activity: HD conversion dropped down to 91%, the outlet concentrations of H_2, CO_2, CO and CH_4 decreased to 56, 18, 5.6 and 0.7 vol. %, respectively. As one can see from Fig. 3a, Rh/CZ demonstrated stable operation for 15 h at 550 °C. It provided 100% conversion of HD with H_2-rich outlet mixture, vol. %: 55 H_2, 16 CO_2, 7 CO and ~ 5 CH_4 approximating the equilibrium composition (Fig. 3c). C_2-C_5 hydrocarbons remained below 0.1 vol. % during the whole experiment. Note that, in contrast to CZA which was inactive in HD SR at 550 °C, CZ itself (before depositing Rh) demonstrated HD conversion of ~5-8% and facilitated the formation of H_2, CO_2 and C1-C5 hydrocarbons in the amount of ca. 2–4, 0.5 and 0.1-0.5 vol. %, respectively (See Supplementary information). That is, the CZ support in the Rh/CZ catalyst is involved in the HD reforming process and serves to improve the catalyst performance.

Thus, the activity and coking resistance of Rh-based catalysts containing alumina are below those values of the catalyst deposited on CZ (Fig. 3) and decrease in the following order: Rh/CZ > Rh/CZB > Rh/CZA-Mg > Rh/CZA. This is in line with the results reported in [23], where steam reforming of n-hexadecane was studied over 21 wt. % Rh/Al_2O_3 and 12 wt. % Rh/CeO_2 supported on microstructured foils. At a temperature of 700 °C, H_2O/C = 4, GHSV = 50,000 h^{-1}, the maximum conversion of n-hexadecane on Rh/Al_2O_3 was 96%. However, the catalysts rapidly lost activity, and the conversion decreased to 65% after 12 h on stream. Rh/CeO_2 showed stable operation under the same conditions [23,24], and provided complete HD conversion after 15 h on stream. At a temperature of 600 °C, Rh/CeO_2 provided a HD conversion of 100% only after the GHSV has been decreased to 25,000 h^{-1}. In our experiments under similar experimental conditions (H_2O/C ~ 3 and GHSV ~ 20,000 h^{-1}), but at a lower reaction temperature (550 °C), complete conversion of n-hexadecane over Rh/CZB and Rh/CZ catalysts was observed during 5 and 16 h, respectively. Taking into account that Rh loading in these catalysts was more than one order of magnitude below that in Rh/Al_2O_3 and Rh/CeO_2 catalysts [23,24], Rh/CZB and Rh/CZ seem to be more promising with respect to steam reforming of n-hexadecane. These catalysts were tested in the next set of experiments under n-hexadecane autothermal reforming conditions.

3.3. Autothermal reforming

Fig. 4 represents the time on stream dependences of HD conversion, H_2, CO and CO_2 concentrations and respective equilibrium values for Rh/CZB and Rh/CZ catalysts in HD ATR at 650 °C and GHSV of 27,000 h^{-1}. It is seen (Fig. 4a) that Rh/CZB demonstrated stable operation,

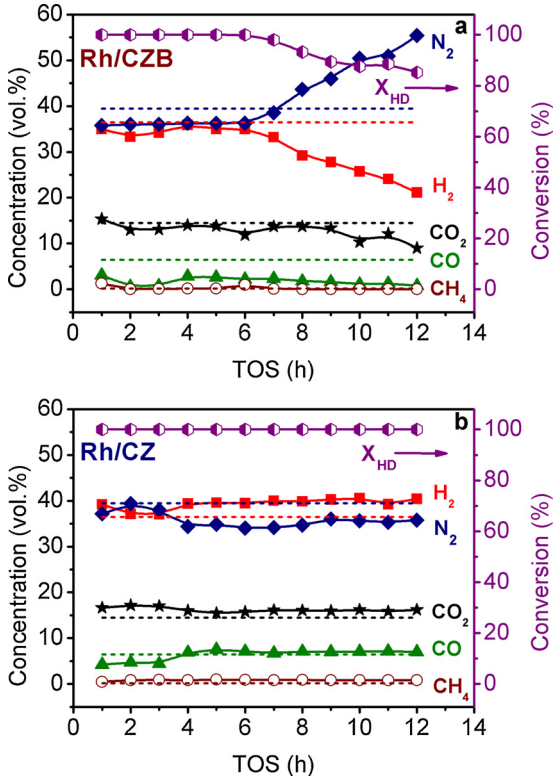

Fig. 4. The HD conversion (a) and product distribution on dry basis (b,c) over Rh/CZB and Rh/CZ in the HD ATR as a function of time on stream at H_2O/C = 2.6, O_2/C = 0.5, T = 650 °C and GHSV = 27,000 h^{-1}. Points – experimental data, dashed lines – equilibrium concentrations.

complete HD conversion and near-equilibrium product distribution only during 6 h on stream. Then the HD conversion and H_2, CO, CO_2 concentrations started to decrease. This process was accompanied by the raise of the outlet concentration of ethane, propane, butane and higher hydrocarbons, which are the intermediate products of HD conversion. Nevertheless, it should be noted that Rh/CZB exhibited high initial activity and provided complete conversion of HD at WHSV of 25,000 $cm^3\,g^{-1}\,h^{-1}$, favorably compared with the literature data [25–27] indicating that diesel ATR catalysts are conventionally operated at ca. 10000-20000 $cm^3\,g^{-1}\,h^{-1}$. Deactivation of Rh/CZB catalyst was associated with the major problem of carbon deposits formation during HD ATR which was confirmed by TPO of the used Rh/CZB (See Section 3.1 and Table 1).

Similarly to HD SR, the Rh/CZ catalyst showed more stable operation in HD ATR at 650 °C than Rh/CZB. Complete HD conversion and near-equilibrium product distribution were observed during 12 h on stream (Fig. 4b). Carbon formation on this catalyst was only 1.5 wt.% (less than on Rh/CZB in HD ATR). On the other hand, the average carbon productivity of Rh/CZ catalyst (Table 1) during HD ATR slightly exceeded that in HD SR. Since total oxidation of HD is highly exothermic reaction, carbon formation may be associated also with hot spot formation at the frontal catalyst bed. It may induce thermal cracking of HD with the formation of unsaturated hydrocarbons. High catalyst heat conductivity is required to provide effective heat transfer. Catalyst deposition onto supports with high heat conductivity is one of the ways to promote its performance in ATR.

3.4. Composite $Rh/Ce_{0.75}Zr_{0.25}O_{2-\delta}$-η-$Al_2O_3$/FeCrAl wire metal mesh catalyst

The novel design of structured Rh/CZB/FCA catalyst was suggested. It was briefly reported in [4], and combined high heat conductivity of

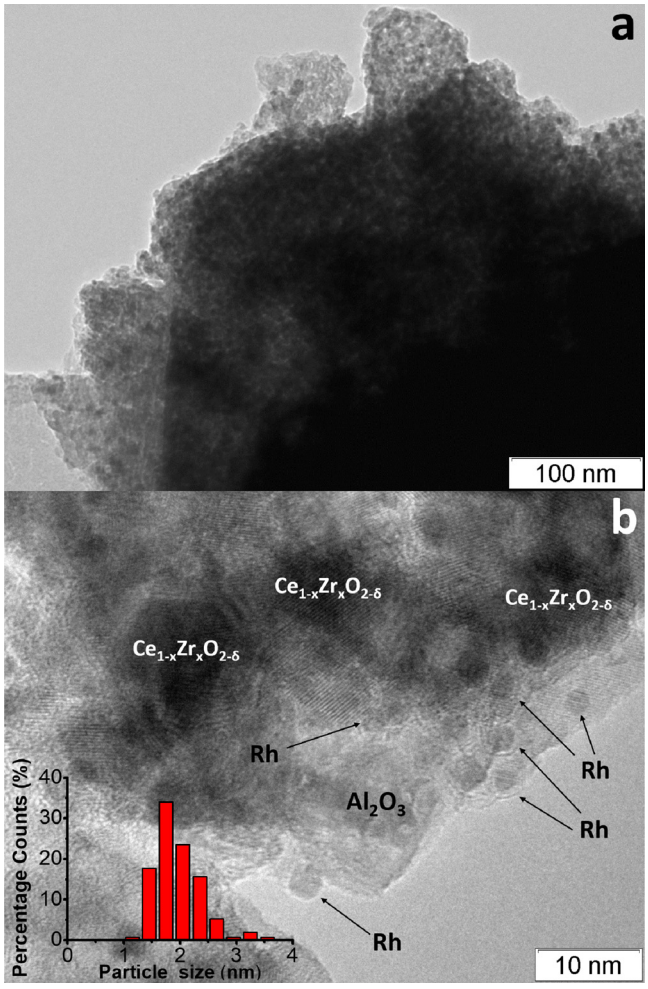

Fig. 5. TEM images of as - prepared Rh/CZB/FCA.

FeCrAlloy wire mesh, high thermal stability, surface area and good adhesion ability of η -Al_2O_3 layer, high coking resistance of ceria-zirconia mixed oxide and high dispersion of Rh nanoparticles. Rh/CZB/FCA was characterized by TEM and SEM techniques.

Fig. 5 presents TEM images of as-prepared Rh/CZB/FCA catalyst. As is seen in Fig. 5a, the support consists of plate-like Al_2O_3 particles of size ~1 μm, bearing on its surface $Ce_{1-x}Zr_xO_{2-\delta}$ crystallites of 5–20 nm size, which form large porous aggregates of a micron scale. The typical interplanar spacing for ceria and zirconia of {111} and {200} planes varies within d = 3.03–3.20 Å and d = 2.65–2.72 Å, respectively, which proves formation of solid solutions of variable composition. The Rh particles exist on the support surface predominantly in a form of 1–2 nm clusters. Some 3–4 nm particles with interplanar distances d = 2.196 Å and d = 1.902 Å corresponding to {111} and {200} planes, respectively, were observed as well (Fig. 5b).

Fig. 6 presents the SEM images of η-Al_2O_3/FeCrAl and Rh/CZB/FCA. As Fig. 6a shows, a layer of η-Al_2O_3 consisted of columnar or needle-shaped crystals (5–10 μm thick, up to 50 μm long) evenly covers the surface of FeCrAl wire mesh. The thickness of η-Al_2O_3 layer is 30–50 μm, as proved by SEM image of a single wire cross-section. Fig. 6b,c present general view of the mesh and SEM images of the surface of as-prepared Rh/CZB/FCA catalyst. After supporting $Rh/Ce_{1-x}Zr_xO_{2-\delta}$ over η-Al_2O_3 layer, the microstructure of the surface has changed. As Fig. 6b shows, the surface of crystals become more rough, while the thickness of the final layer remained the same (30–50 μm).

According to EDX data for several 100 x 100 μm areas, the surface of Rh/CZB/FCA contains Rh, Ce, Zr, Al, and O. Concentrations of the elements throughout all areas were similar that proves uniform

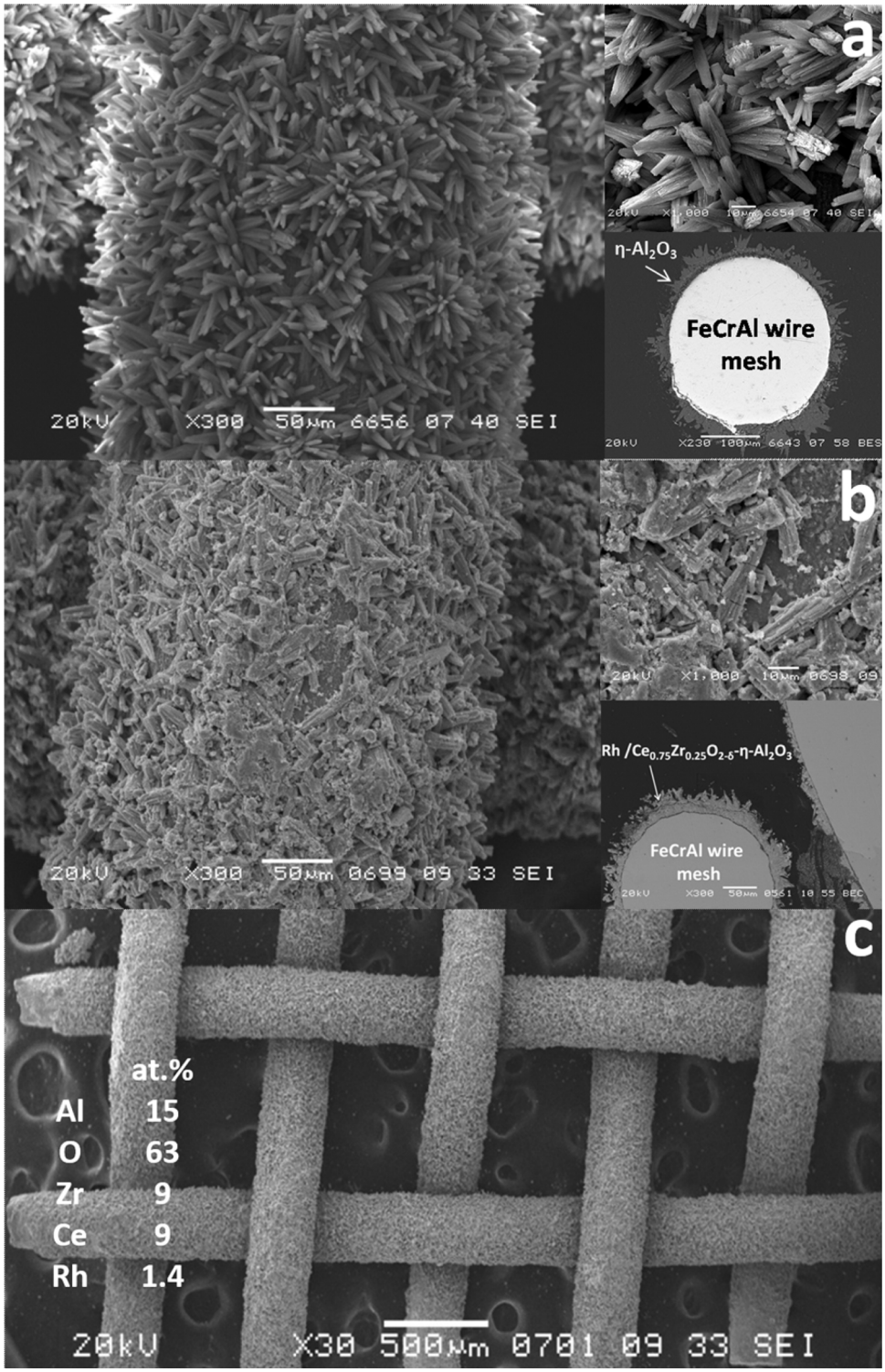

Fig. 6. SEM images of η-Al_2O_3/FeCrAl (a) and as - prepared Rh/CZB/FCA (b,c) catalyst.

distribution of Rh and $Ce_{1-x}Zr_xO_{2-\delta}$ over the surface of η-Al_2O_3 crystals, in good agreement with TEM data.

Thus, the structured Rh/CZB/FCA catalyst is a composite in which alumina, chemically bound with the metal substrate, provides mechanical strength of the catalytic layer and preserves Rh and $Ce_{1-x}Zr_xO_{2-\delta}$ in dispersed state.

Rh/CZB/FCA was studied in HD ATR. Fig. 7 represents the time on stream dependences of HD conversion, H_2, CO CO_2, N_2, CH_4 and C2-C5 hydrocarbon concentrations and respective equilibrium values for HD ATR over Rh/CZB/FCA catalyst at 550–650 °C and WHSV of 38,500 - 115,500 $cm^3\,g^{-1}\,h^{-1}$. It is seen that Rh/CZB/FCA demonstrated stable operation for 4 h, providing complete HD conversion and equilibrium product distribution in Region A (T = 650 °C, WHSV = 38,500 $cm^3\,g^{-1}\,h^{-1}$). No C2-C5 hydrocarbons were observed among the reaction products.

A two-fold increase in the flow rate (Region B: T = 650 °C, WHSV = 77,000 $cm^3\,g^{-1}\,h^{-1}$) produced no effect on HD conversion and outlet concentrations. The catalyst demonstrated stable operation

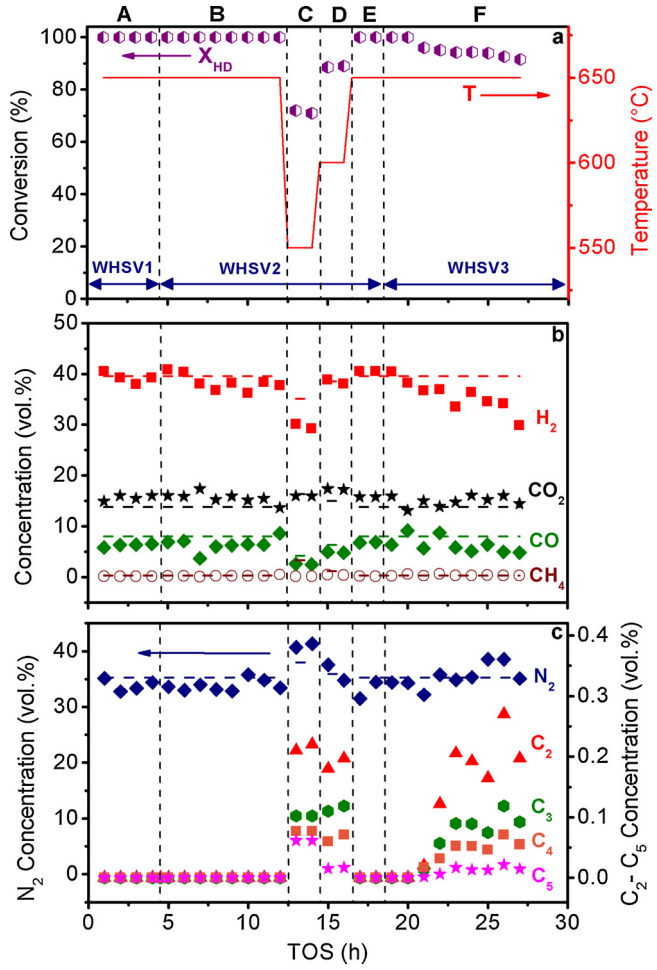

Fig. 7. The HD conversion and temperature (a), product distribution on dry basis (b,c) over Rh/CZB/FCA, in the HD ATR as a function of time on stream at $H_2O/C = 2.6$, $O/C = 0.4$. and WHSV = 38,500 (Region A); 77,000 (Region B–E); 115,500 $cm^3\,g^{-1}\,h^{-1}$ (Region F). Points – experimental data, dashed lines – equilibrium concentrations.

during 8 h.

As the temperature was decreased to 550 °C (Region C), the HD conversion came down to 72%; the outlet concentrations of H_2 and CO decreased to 35 and 4 vol.%, respectively. C2-C5 hydrocarbons were detected in the outlet mixture in total concentration not exceeding 0.5 vol.%.

Further elevation of the temperature to 600 and then to 650 °C (Regions D and C) caused the increase in HD conversion to 90 and 100%, respectively. Concentrations of the reaction products returned to the initial values observed during the first 12 h of the catalyst operation (Regions A, B).

In Region F (WHSV = 115,500 $cm^3\,g^{-1}\,h^{-1}$, 650 °C), complete HD conversion and almost equilibrium concentrations of the reaction products were observed during 2 h. Then, during the next 7 h X_{HD} lowered to 92%; H_2 and CO outlet concentrations decreased to 30 and 5 vol.%, respectively, whereas N_2 concentration increased to 37%. The concentrations of CH_4 and CO_2 changed insignificantly. The decrease in HD conversion was accompanied by increasing content of C2-C5 hydrocarbons in the outlet gas mixture, but their total concentration remained below 0.5 vol.%.

No damages of Rh/$Ce_{0.75}Zr_{0.25}O_{2-\delta}$-η-$Al_2O_3$ coating were identified after 30 h on stream that confirms good adhesion of catalytic coating even under severe reaction conditions with high temperature gradients and flow changes.

The amount of carbon formed after 27 h on stream was only 1.5 wt. % that corresponded to average carbon productivity of 0.3 $g_C \cdot kg_{HD}^{-1} \cdot g_{cat}^{-1}$. This value is much less than that of any alumina containing samples (Table 1) and even Rh/CZ in both HD SR and ATR. We associate good coking resistance of Rh/CZB/FCA catalyst with high heat conductivity of FeCrAl alloy wire mesh that prevents thermal cracking of HD; high Rh dispersion and oxygen mobility in $Ce_{0.75}Zr_{0.25}O_{2-\delta}$ and blocking of η-Al_2O_3 acidic surface sites during 7-step impregnation with Ce and Zr precursors that minimizes carbon formation on the catalyst surface.

So, as is seen in Fig. 7, Rh/CZB/FCA demonstrated an outstanding performance in HD ATR providing a 100% conversion at WHSV of 77,000 $cm^3\,g^{-1}\,h^{-1}$ (with respect to weight of Rh/$Ce_{0.75}Zr_{0.25}O_{2-\delta}$-η-$Al_2O_3$ coating) and H_2 production rate of 2.2 $kg_{H_2}\,kg_{cat}^{-1}h^{-1}$. This productivity is more than three times exceeds respective value calculated from the data previously reported for 0.3 wt%Rh/3 wt%MgO/20 wt %CeO_2-ZrO_2 supported on cordierite monolith studied in n-octane ATR under close reaction conditions [28]. Rh/CZB/FCA strongly surpasses all powdered catalysts tested in the present work. High performance of the catalyst was achieved due to a combination of high heat conductivity of FeCrAl alloy wire mesh and high Rh dispersion in the coating layer.

4. Conclusions

The performance in HD SR and ATR of three well-characterized alumina-modified samples was compared with that of Rh/$Ce_{0.75}Zr_{0.25}O_{2-\delta}$ catalyst with similar Rh dispersion. Composite Rh/$Ce_{0.75}Zr_{0.25}O_{2-\delta}$-η-$Al_2O_3$/FeCrAl wire metal mesh catalyst was examined in HD ATR. The main observations are as follows:

- Alumina additive (no matter how in was introduced) increases the surface area and thermal stability of Rh/CZ catalysts and maintain high Rh dispersion.
- Addition of alumina deteriorates the catalyst performance in HD SR and ATR due to enhancement of coking processes. Catalyst treatment with $Mg(OAc)_2$ significantly slows down the coking process, indicating alumina surface acidic sites to be responsible for undesired side reactions.
- Catalysts coking productivity under HD ATR conditions is higher than that under HD SR conditions. It is most likely associated with the contribution of thermal cracking reactions induced by hot spots at the front of the catalyst bed.
- Composite Rh/$Ce_{0.75}Zr_{0.25}O_{2-\delta}$-η-$Al_2O_3$/FeCrAl wire metal mesh catalyst surpasses other samples tested in terms of activity and coking resistance owing to high heat conductivity of FeCrAl alloy wire mesh, high Rh dispersion, oxygen mobility in $Ce_{0.75}Zr_{0.25}O_{2-\delta}$ oxide and blocking of η-Al_2O_3 acidic surface sites during ceria-zirconia deposition procedure.

Acknowledgement

The work was conducted within the framework of budget project #AAAA-A17-117041710088-0 for Boreskov Institute of Catalysis.

Appendix A. Supplementary data

Supplementary material related to this article can be found, in the online version, at doi:https://doi.org/10.1016/j.apcatb.2018.12.037.

References

[1] J. Bae, S. Lee, S. Kim, J. Oh, S. Choi, M. Bae, I. Kang, S.P. Katikaneni, Liquid fuel processing for hydrogen production: a review, Int. J. Hydrogen Energy 41 (2016) 19990–20022.

[2] M.Z. Granlund, K. Jansson, M. Nilsson, J. Dawody, L.J. Pettersson, Evaluation of Co, La, and Mn promoted Rh catalysts for autothermal reforming of commercial diesel : aging and characterization, Appl. Catal. B 172–173 (2015) 145–153.

[3] M.Z. Granlund, K. Jansson, M. Nilsson, J. Dawody, L.J. Pettersson, Evaluation of Co, La, and Mn promoted Rh catalysts for autothermal reforming of commercial diesel, Appl. Catal. B 154 (2014) 386–394.
[4] T.B. Shoynkhorova, V.N. Rogozhnikov, P.A. Simonov, P.V. Snytnikov, A.N. Salanov, A.V. Kulikov, E.Y. Gerasimov, V.D. Belyaev, D.I. Potemkin, V.A. Sobyanin, Highly dispersed Rh/$Ce_{0.75}Zr_{0.25}O_{2-\delta}$-η-$Al_2O_3$/FeCrAl wire mesh catalyst for autothermal n-hexadecane reforming, Mater. Lett. 214 (2018) 290–292.
[5] X. Karatzas, K. Jansson, J. Dawody, R. Lanza, L.J. Pettersson, Microemulsion and incipient wetness prepared Rh-based catalyst for diesel reforming, Catal. Today 175 (2011) 515–523.
[6] T.B. Shoynkhorova, P.A. Simonov, D.I. Potemkin, P.V. Snytnikov, V.D. Belyaev, A.V. Ishchenko, D.A. Svintsitskiy, V.A. Sobyanin, Sorption-hydrolytic deposition for diesel fuel reforming to syngas, Appl. Catal. B 237 (2018) 237–244.
[7] S. Yoon, I. Kang, J. Bae, Effects of ethylene on carbon formation in diesel auto-thermal reforming, Int. J. Hydrogen Energy 33 (2008) 4780–4788.
[8] P. Avila, M. Montes, E.E. Miró, Monolithic reactors for environmental applications: a review on preparation technologies, Chem. Eng. J. 109 (2005) 11–36.
[9] X. Karatzas, J. Dawody, A. Grant, E.E. Svensson, L.J. Pettersson, Zone-coated Rh-based monolithic catalyst for autothermal reforming of diesel, Appl. Catal. B 101 (2011) 226–238.
[10] A.V. Porsin, A.V. Kulikov, V.N. Rogozhnikov, A.N. Serkova, A.N. Salanov, K.I. Shefer, Structured reactors on a metal mesh catalyst for various applications, Catal. Today 273 (2016) 213–220.
[11] A.V. Porsin, V.N. Rogoznikov, A.V. Kulikov, A.N. Salanov, A.N. Serkova, Crystallization of aluminum hydroxide in a sodium aluminate solution on a heterogeneous surface, Cryst. Growth Des. 17 (2017) 4730–4738.
[12] S. Zhao, J. Zhang, D. Weng, X. Wu, A method to form well-adhered γ-Al_2O_3 layers on FeCrAl metallic supports, Surf. Coat. Technol. 167 (2003) 97–105.
[13] M. Valentini, G. Groppi, C. Cristiani, M. Levi, E. Tronconi, P. Forzatti, The deposition of γ-Al_2O_3 layers on ceramic and metallic supports for the preparation of structured catalysts, Catal. Today 69 (2001) 307–314.
[14] A. Trovarelli, Catalytic properties of ceria and CeO_2-containing materials, Catal. Rev. - Sci. Eng. 38 (1996) 439–520.
[15] F. Lin, A. Wokaun, I. Alxneit, Rh-doped Ceria: solar organics from H_2O, CO_2 and sunlight, Energy Procedia 69 (2015) 1790–1799.
[16] E.A. Alikin, S.P. Denisov, N.M. Danchenko, V.N. Rychkov, A.S. Volkov, A.S. Karpov, Thermally stable composite system Al_2O_3 – $Ce_{0.75}Zr_{0.25}O_2$ for automotive three way catalysts, Catal. Ind. 5 (2013) 133–142.
[17] P.A. Simonov, T.B. Shoynkhorova, P.V. Snytnikov, D.I. Potemkin, V.D. Belyaev, V. A. Sobyanin, Method of catalyst preparation, Russian Patent №2653360, published 08.05.2018.
[18] L. Wu, B.E. Schwederski, D.W. Margerum, Stepwise hydrolysis kinetics of tetra-chloroplatinate (II) in base, Inorg. Chem. 29 (1990) 3578–3584.
[19] D. Kashchiev, G.M. van Rosmalen, Review: nucleation in solutions revisited, Cryst. Res. Technol. 38 (2003) 555–574.
[20] J. Freel, Chemisorption on supported platinum, J. Catal. 25 (1972) 139–148.
[21] B.C. Gates, J.R. Katzer, G.C.A. Schuit, Chemistry of Catalytic Processes, McGraw-Hill, New York, 1979.
[22] C. Naccache, Deactivation and Poisoning of Catalysts, Marcel Dekker, New York, 1985.
[23] J. Thormann, P. Pfeifer, U. Kunz, K. Schubert, Reforming of diesel fuel in a Micro reactor, Int. J. Chem. React. Eng. 6 (2008) art. no. P1.
[24] J. Thormann, L. Maier, P. Pfeifer, U. Kunz, O. Deutschmann, K. Schubert, Steam reforming of hexadecane over a Rh/CeO_2catalyst in microchannels: experimental and numerical investigation, Int. J. Hydrogen Energy 34 (2009) 5108–5120.
[25] W.S. Lee, D.G. Ju, S.Y. Jung, S.C. Lee, D.S. Ha, B.W. Hwang, J.C. Kim, N-dodecane autothermal reforming properties of Ni-Al based catalysts prepared by various methods, Top. Catal. 60 (2017) 727–734.
[26] M.C. Alvarez-Galvan, R.M. Navarro, F. Rosa, Y. Bricen, F.G. Alvarez, J.L.G. Fierro, Performance of La, Ce-modified alumina-supported Pt and Ni catalysts for the oxidative reforming of diesel hydrocarbons, Int. J. Hydrogen Energy 33 (2008) 652–663.
[27] S.Y. Jung, D.G. Ju, E.J. Lim, S.C. Lee, B.W. Hwang, J.C. Kim, Study of sulfur-resistant Ni-Al-based catalysts for autothermal reforming of dodecane, Int. J. Hydrogen Energy 40 (2015) 13412–13422.
[28] A. Qi, S. Wang, C. Ni, D. Wu, Autothermal reforming of gasoline on Rh-based monolithic catalyst, Int. J. Hydrogen Energy 32 (2007) 981–991.